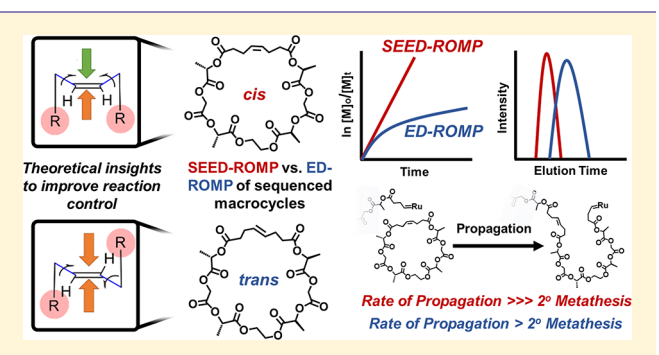


Sequence-Controlled Polymers Through Entropy-Driven Ring-Opening Metathesis Polymerization: Theory, Molecular Weight Control, and Monomer Design

Jamie A. Nowalk, Cheng Fang, Amy L. Short, Ryan M. Weiss, Jordan H. Swisher, Peng Liu, Feng Liu, and Tara Y. Meyer*,†,‡

Supporting Information

ABSTRACT: The bulk properties of a copolymer are directly affected by monomer sequence, yet efficient, scalable, and controllable syntheses of sequenced copolymers remain a defining challenge in polymer science. We have previously demonstrated, using polymers prepared by a step-growth synthesis, that hydrolytic degradation of poly(lactic-co-glycolic acid)s is dramatically affected by sequence. While much was learned, the step-growth mechanism gave no molecular weight control, unpredictable yields, and meager scalability. Herein, we describe the synthesis of closely related sequenced polyesters prepared by entropy-driven ring-opening metathesis polymerization (ED-ROMP) of strainless macromonomers with im-



bedded monomer sequences of lactic, glycolic, 6-hydroxy hexanoic, and syringic acids. The incorporation of ethylene glycol and metathesis linkers facilitated synthesis and provided the olefin functionality needed for ED-ROMP. Ring-closing to prepare the cyclic macromonomers was demonstrated using both ring-closing metathesis and macrolactonization reactions. Polymerization produced macromolecules with controlled molecular weights on a multigram scale. To further enhance molecular weight control, the macromonomers were prepared with cis-olefins in the metathesis-active segment. Under these selectivity-enhanced (SEED-ROMP) conditions, first-order kinetics and narrow dispersities were observed and the effect of catalyst initiation rate on the polymerization was investigated. Enhanced living character was further demonstrated through the preparation of block copolymers. Computational analysis suggested that the enhanced polymerization kinetics were due to the cis-macrocyclic olefin being less flexible and having a larger population of metathesis-reactive conformers. Although used for polyesters in this investigation, SEED-ROMP represents a general method for incorporation of sequenced segments into molecular weightcontrolled polymers.

INTRODUCTION

There exists a clear demand for the development of general, scalable, and controllable synthetic methods for imbedding monomer sequence in synthetic copolymers both to enable the production of novel materials for applications and also to define more clearly how sequence controls properties. The effects of monomer sequence on polymer properties are wellestablished in Nature, wherein precise monomer order can be directly mapped to macromolecular function. In synthetic polymer chemistry, in contrast, sequence control and the derivation of structure/function relationships have been limited to a variety of more easily accessible motifs including alternating, gradient, or blocky structures. 1-3 The attainment of a more detailed understanding has been inhibited by the

challenges inherent in preparing precisely sequenced copolymers with molecular weight control. In the few classes of materials for which data have been obtained, the majority of the work has focused on solution phase properties; the most studied systems include peptoids, 4,5 foldamers, 6-8 and systems exploiting molecular recognition moieties. 9-11 Bulk-phase structure/function studies, which typically require gram-scale quantities, 12 are extremely rare. 4,13-23

Our group has long been interested in understanding the connections between sequence and properties in nonbiological polymers. In the course of that work we have developed

Received: December 7, 2018 Published: February 4, 2019



[†]Department of Chemistry, University of Pittsburgh, Pittsburgh, Pennsylvania 15260, United States

^{*}McGowan Institute for Regenerative Medicine, University of Pittsburgh, Pittsburgh, Pennsylvania 15219, United States

[§]Computational Modeling & Simulation Program, University of Pittsburgh, Pittsburgh, Pennsylvania 15260, United States

⁵Department of Chemical and Petroleum Engineering, University of Pittsburgh, 3700 O'Hara Street, Pittsburgh, Pennsylvania 15261, United States

synthetic routes to periodically sequenced poly(lactic-coglycolic acid)s (PLGA)s and established that bulk phase behaviors during hydrolysis are extremely dependent on constituent monomer sequence.^{24–26} Our interest in this class of polymers and their behavior arose because of their potential for application as degradable sutures, drug delivery vehicles, and cell scaffolds. ^{27–32} The random version of this class of polymer, which is widely used and FDA-approved, exhibits a degradation profile that is controlled primarily by molecular weight and the ratio of lactic (L) to glycolic acid (G) monomers.²⁸ Our work on periodic PLGAs demonstrated that monomer sequence is an even more powerful tool for controlling hydrolysis behavior, facilitating not only rate control, but also affecting the retention of mechanical properties, swelling, internal pH, lactic acid release, and release of guest molecules in vitro.2

Despite our successes in carrying out structure/function studies on sequenced PLGAs, the scalable and controllable syntheses of these polymers remained an ongoing challenge. Our original synthetic efforts relied on materials prepared by a step-growth synthesis in which hydroxy-acid sequenced oligomers (segmers) were first prepared and then polymerized. Using this segmer-assembly polymerization (SAP) method, we were able to prepare a large range of periodic copolymers. Although moderately scalable, SAP provided no molecular weight control, unpredictable yields, poor reproducibility, and relatively large dispersities ($\bar{D} = 1.5 - 1.8$). These issues limited the accuracy and scope of structure/function studies for these materials.

To address these synthetic limitations, we sought to develop a general method of preparing sequence-controlled polymers that proceeded, at least initially, via a chain-mechanism pathway. Specifically, we targeted entropy-driven ring-opening metathesis polymerization (ED-ROMP), which has been used previously to polymerize cyclic macromonomers.33-42 We sought to prepare sequenced macrocyclic oligomers (MCOs) containing LG segments, a "linker" monomer to connect these segments that would not dominate bulk properties, 43 and an olefin-metathesis site (Scheme 1). This new polymerization approach was expected to improve molecular weight control, decrease dispersity, and achieve higher molecular weights than those obtained by the step-growth SAP methodology. In previous communications, 44,45 we reported our initial successes using this approach. Herein, we describe in detail how ED-ROMP functions in this system and how we were able to introduce living character into the polymerization through a simple trans- to cis-olefin substitution.

ED-ROMP has been used previously to polymerize strainless macrocycles, typically containing greater than 14 atoms, with entropy serving as the primary driving force (Figure 1).³³ High concentration is used to favor polymer chains over cyclic species. The molecular weight and dispersity observed at any time point depend on the rate of propagation $(k_{\rm pr})$ relative to that of secondary metathesis $(k_{\rm sm})$. It should be noted that termination reactions are not typically observed in these systems on the time scale of a normal polymerization. Final molecular weights and dispersities are a function of monomerto-catalyst loading ([M]/[cat]), ring-chain equilibrium, and overall concentration. 33,49 ED-ROMP typically results in dispersities greater than 1.1 due to competing secondary metathesis/backbiting (chain-transfer) reactions.

Although unmodified ED-ROMP does allow for molecular weight control, the prevalence of secondary metatheses of the

Scheme 1. Overall Synthetic Approach Involving Ring-Closing to Prepare Macrocycles with Embedded Monomer Sequences and Sequence-Retaining Metathesis Polymerization

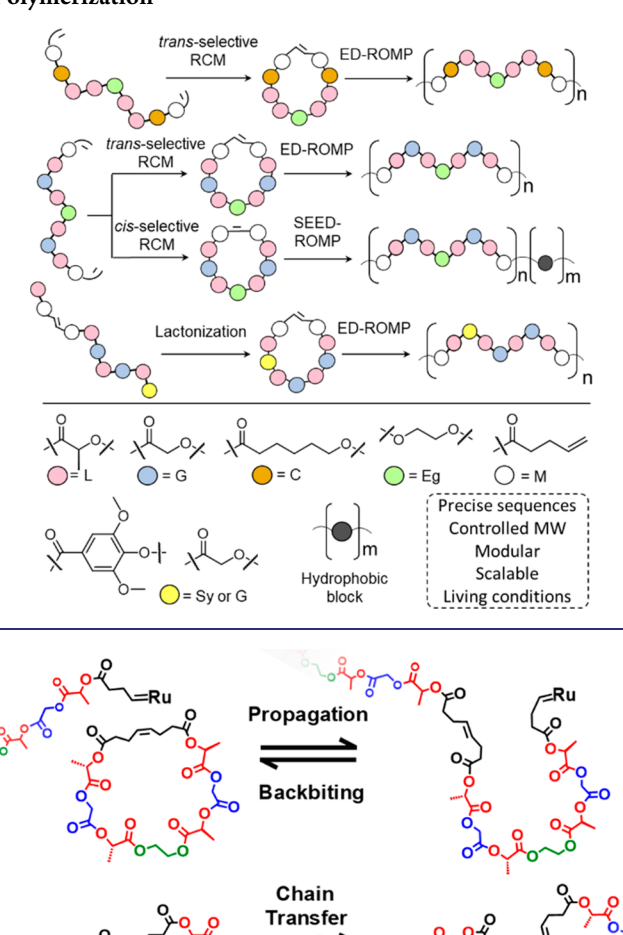


Figure 1. Living character as a function of the relative rates of propagation (k_{pr}) and secondary metathesis (k_{sm}) in entropy-driven ring-opening metathesis polymerization.

Propagation

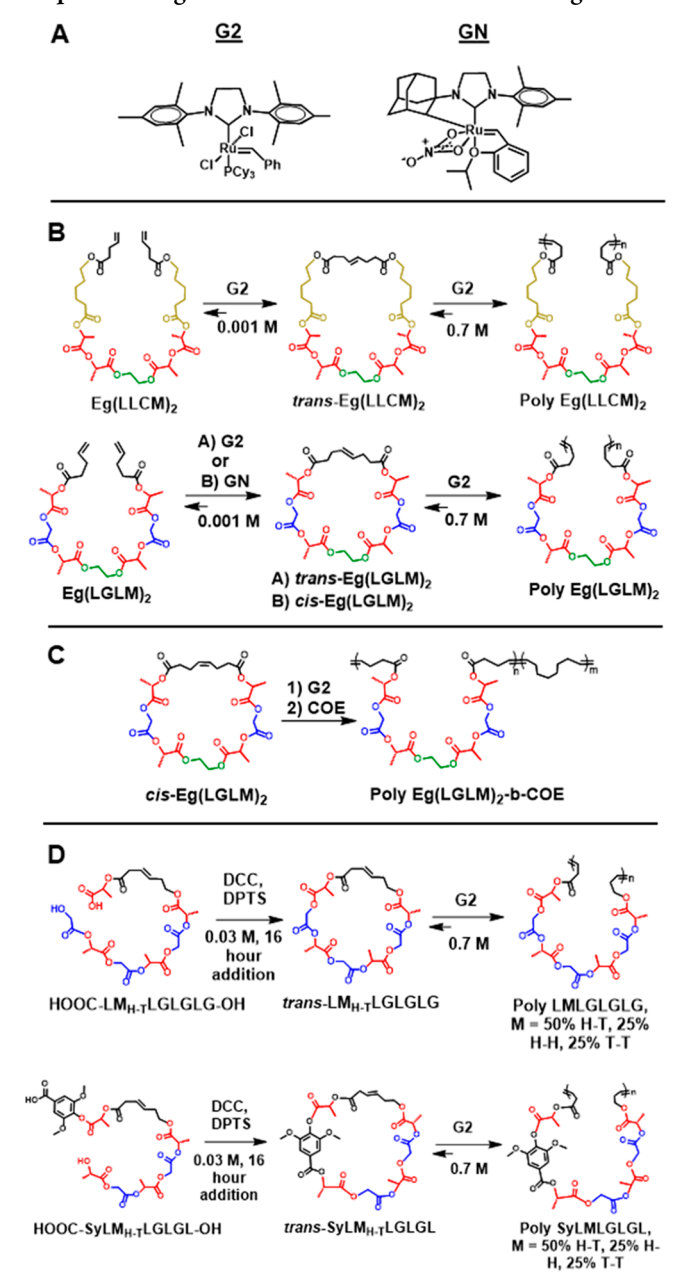
Backbiting Chain Transfer

newly produced olefin backbone interferes with the ideal behavior that would be expected for a system in which $k_{\rm pr}$ is much greater than $k_{\rm sm}$. Such a system would be expected to behave in a more "living" fashion, giving chains that grow steadily and similarly in molecular weight.

Knowing that these rates depend on the steric accessibility of the olefin, 50 we have chosen to investigate, both theoretically and experimentally, the effects of the olefin geometry on mechanism and living character. Our findings culminate in the description of a new variant that we term Selectivity-Enhanced ED-ROMP, or SEED-ROMP. The MCOs used in these studies consist of strainless rings equipped with metathesisactive olefin linkers (M). Each MCO also incorporates sequences of lactic (L), glycolic (G), 6-hydroxy hexanoic (C), and syringic (Sy) acids as well an ethylene glycol (Eg)

unit for palindromic monomers (Scheme 2). For some MCOs the polymerizations are studied as a function the *cis/trans*

Scheme 2. Ring-Closing and Polymerization Reactions of Sequenced Segmers for Controlled Molecular Weight^a



^a(A) Grubbs second generation (G2) and nitrato Grubbs (GN) catalyst structures. (B) Ring-closing metathesis and ensuing polymerizations of Eg(LLCM)₂ and Eg(LGLM)₂ segmers. (C) Selectivity-enhanced entropy-driven ring-opening metathesis polymerization to prepare poly (EgLGLM)₂-b-COE. (D) Macrolactonization reactions of LMLGLGLG and SyLMLGLGL and subsequent polymerizations.

content of the metathesis linker. The differential behavior of these species is also investigated computationally with the goal of understanding the increased living character observed for the *cis*-SEED-ROMP monomers.

RESULTS AND DISCUSSION

Synthesis. Detailed information on the synthesis of MCOs and polymerization conditions is provided in the Supporting Information (SI). L-Lactic acid is the isomer used throughout. The synthesis of MCOs in this work are derived from protocols previously reported by our group for the production of sequenced oligomers of α -hydroxy acids. $^{24-26,51}$ A typical synthesis begins with orthogonal protections of monomers acid moieties with benzyl (Bn) groups and alcohols with tertbutyldiphenylsilyl (TBDPS) groups. Ester couplings with dicvclohexylcarbodiimide (DCC) and nucleophilic amine catalyst DPTS provide diprotected hydroxy-acids which are named from the acid-terminus to alcohol-terminus. Removal of the Bn group via hydrogenolysis provides free acids and removal of the TBDPS group with TBAF provides free alcohols that are then available for sequential cycles of couplings and deprotection. Under these reaction conditions little or no transesterification is observed.

MCOs trans-Eg(LGLM)₂ and trans-Eg(LLCM)₂ were prepared by symmetric coupling of trimeric sequences of the specified hydroxy-acids to Eg. The resulting diols were coupled to 4-pentenoic acid to give an acyclic diene. Ring-closing metathesis (RCM) with Grubbs second-generation catalyst (G2) provided the MCO products in excellent yield, with ~90% trans-selectivity. These oligomers may also be ring-closed in the presence of Grubbs Z-selective nitrato catalyst (GN)⁵² with the exact opposite selectivity. MCO cis-Eg(LGLM)₂ was obtained in this fashion. The RCM reactions are highly reproducible but require extremely low concentrations (0.001 M) and 10–15 mol % catalyst loadings.⁵³

Although the palindromic monomers were moderately scalable, we were able both to improve scalability and remove the **Eg** unit by desymmetrizing the open-chain oligomer and incorporating the olefin as an intact unit. This method, which exploits macrolactonization⁵⁴ to achieve the ring-closing, benefits from eliminating the large ruthenium catalyst loadings required for RCM and can be used to obtain similar yields using 30× less solvent.

Additionally, the nonsymmetrical monomers provide linkage directionality more closely resembling virgin PLGAs with acid and alcohol termini. In this fashion, hydroxy-acid sequenced precursors **LMLGLGLG** and **SyLMLGLGL** were ring-closed at low concentration at 60 °C in dichloroethane charged with DCC and DPTS. Slow addition of the oligomer over the course of 16 h provided the desired product in yields >85%. Polymerization of these MCOs produced polymers with a conservation of order within each MCO-derived segment but head—tail disorder at the olefin connector as evidenced by ¹H NMR spectroscopy (Figure 2A).

All ED-ROMPs or SEED-ROMPs were performed at 0.7 M at RT with G2 catalyst loadings ranging from 1 to 5 mol % resulting in 20–80 kDa across the four MCOs (Table 1).

As the residual ruthenium remaining in the polymers is a common problem for products of metathesis whose primary application is in the field of regenerative medicine, polymers were purified using a combination of reprecipitation and exposure to a thiol-functionalized resin. ⁵⁵,56 Using this method, concentrations of ruthenium in the polymer matrix were reduced from 1200 to 34 ppm, approaching acceptable levels for most biological applications. ⁵⁷,58

Syringic Acid Incorporation to Elevate T_g . As the ED-ROMP of M-containing MCOs produced polymers with T_g s of

Journal of the American Chemical Society

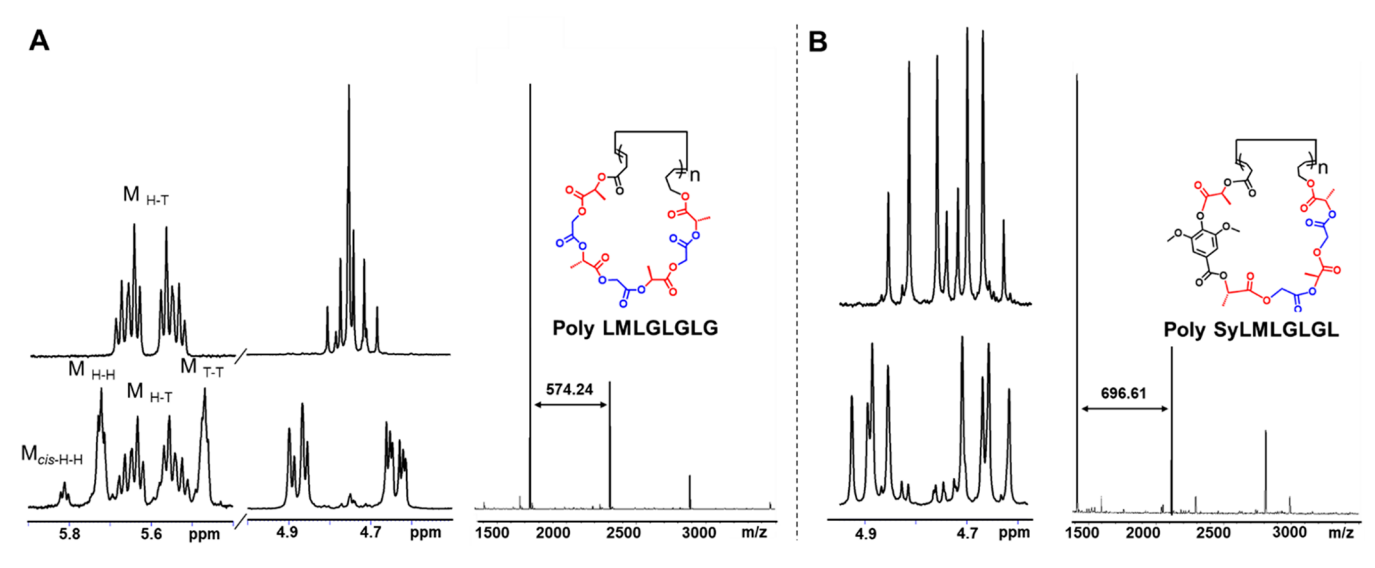


Figure 2. ¹H NMR spectroscopy and MALDI-TOF mass spectrometry characterization of sequence fidelity. (A) NMR spectra of olefin and methylene resonances of *trans-LMLGLGLG* (top) and *Poly LMLGLGLG* (bottom), displaying head—tail olefin resonances, and MALDI-TOF spectrum of low molecular weight cyclic *Poly LMLGLGLG*. (B) ¹H NMR methylene resonances of *trans-SyLMLGLGL* (top) and *Poly SyLMLGLGL* (bottom); and MALDI-TOF spectrum of low molecular weight cyclic *Poly SyLMLGLGL*.

Table 1. Polymer Thermal Data and Molecular Weights

polymer	M/cat	$T_{\rm g} ({\rm oC})^a$	M_n (kDa)	M _w (kDa)	Đ
Poly Eg(LLCM) ₂	20	-11	24 ^b	32 ^b	1.3 ^b
8(/2	45		42 ^b	53 ^b	1.3 ^b
	75		48 ^b	63 ^b	1.3 ^b
	125		60 ^b	78 ^b	1.3 ^b
Poly Eg(LGLM) ₂ ^d	78	18	33 ^c	44 ^c	1.3 ^c
	33		36 ^c	41 ^c	1.1°
	80		56 ^c	58 ^c	1.0 ^c
	90		66 ^c	68 ^c	1.0 ^c
	100		70^c	71 ^c	1.0°
Poly LMLGLGLG	33	20	26 ^c	34 ^c	1.5°
	50		30 ^c	42 ^c	1.4 ^c
	57		33 ^c	47 ^c	1.4 ^c
	67		33 ^c	45°	1.4 ^c
	80		42 ^c	55 ^c	1.3°
	100		43°	55 ^c	1.3°
Poly SyLMLGLGL	80	50	36 ^c	44 ^c	1.2°
	100		44 ^c	51 ^c	1.2 ^a

"Second heating cycle at 10 °C/min. "SEC in THF, absolute molecular weight data. "SEC in THF, relative to PS standards."

"Prepared by SEED-ROMP from cis-Eg(LGLM)₂.

18–20 °C, which are lower than that required for most biomedical applications ($\sim 40-50$ °C), we exploited the modular nature of the synthetic method to incorporate a biocompatible monomer that would elevate $T_{\rm g}.$ We were inspired by the Miller group to include syringic acid (Sy), a phenolic acid antioxidant found in grains and plant cell walls. 43,59 Thus, the segmer SyLMLGLGL was ring-closed via lactonization, and polymerized to prepare Poly SyLMLGLGL with $M_{\rm n}{\rm s}$ up to 45 kDa. The polymer exhibited the targeted increase in $T_{\rm g}$ (50 °C).

Sequence Characterization. The exquisite sensitivity of the diastereotopic G methylene protons provide a fingerprint of sequence in ¹H NMR spectra (Figure 2). We have previously determined that in some instances the chemical shifts of these protons are affected by sequence differences up to six monomer units away, and as little as 2% sequence error

can be easily resolved.⁶⁰ As such, we are able to clearly characterize and differentiate copolymers with a range of structures. In addition to general characterization and confirmation of sequence, this sensitivity also makes it possible to monitor quantitatively the progress of the polymerization reaction as a function of time and isomer.

The palindromic MCOs provided the simplest spectra. Pairs of doublets in which *cis*- and *trans*-olefin composition can be monitored allowed us to monitor RCM conformational selectivity and polymerization kinetics (Figure 3). The unsymmetric MCOs obtained via macrolactonization displayed more complex methylene resonances, yet ring-opened chains could still be fully distinguished from monomer (Figure 2).

Neither *trans*-LM_{H-T}LGLGLG nor *trans*-SyLM_{H-T}LGLGL polymerized regioselectively. Thus, a statistical distribution of head—tail connectivities of 50% head—tail M_{H-T}, 25% head—head M_{H-H}, and 25% tail—tail M_{T-T} resulted, as evidenced by the distinct ¹H NMR olefin signals (Figure 2A). This analysis confirms that the selected M linker is long enough to eliminate local electronic effects of constituent monomers. We hypothesize that the selectivity could be improved by using a trisubstituted olefin although those experiments were not performed in this study. ^{38,61-65} The conversion of *trans*-SyLMLGLGL to Poly SyLMLGLGL can be followed spectroscopically (Figure 2B).

MALDI-TOF Sequence Characterization. In addition to NMR spectroscopy as a sequence characterization tool, we have previously demonstrated the power of MALDI-TOF mass spectrometry to characterize the fidelity of sequenced polyesters, even in cases where only the most volatile shorter chains in the distribution are observed. In the currently reported ED-ROMP copolymers, a similar analysis consists primarily of chains whose molecular weights are multiples of the MCO masses (Figure 2). Peaks for sequence errors that either add, omit, or substitute monomers within repeat units are weak or not observed.

cis- vs trans-Olefin Studies. Our original MCO trans-Eg(LGLM)₂, prepared via RCM with G2, consisted of 85– 90% trans-isomer. Polymerization kinetics were monitored by

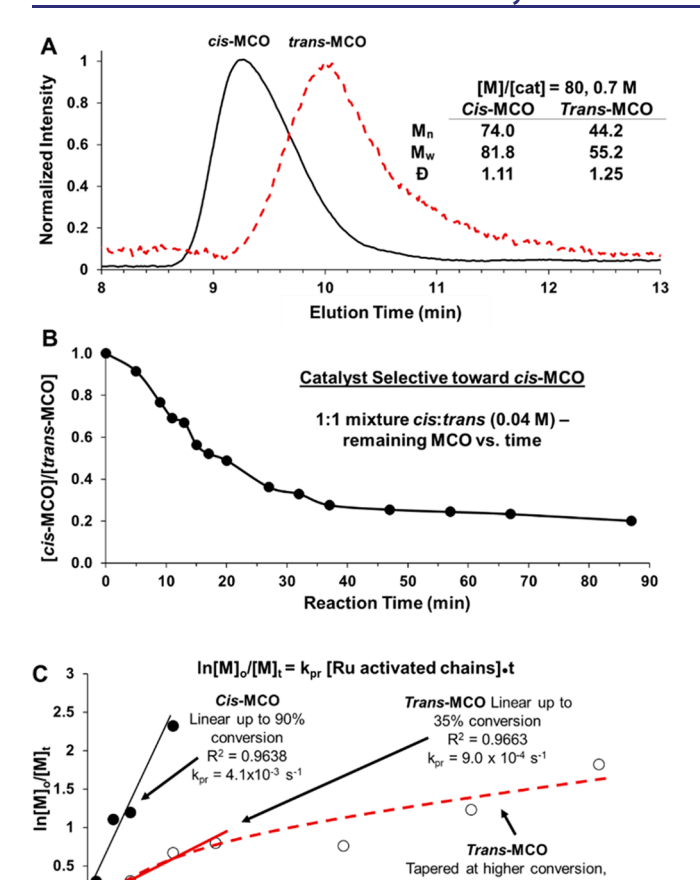


Figure 3. Comparison of *trans*- versus *cis*-Eg(LGLM)₂ polymerizations. (A) SEC traces and molecular weight data for polymerizations with identical catalyst loadings. (B) Catalyst competition experiment with 1:1 *trans:cis* olefin mixture upon exposure to Grubbs second generation catalyst over time, 0.04 M. (C) First-order kinetic fits of *trans*- (both low and high conversions) and *cis*-Eg(LGLM)₂ assuming saturation conditions.

2000

Time (s)

2500

500

1000

1500

indicative of chain transfer

4000

3500

 1 H NMR spectroscopy. *trans*-Olefin content in the resulting polymer remained at ~85% at all times during the polymerization. Molecular weight stabilized in approximately 30 min with dispersities of ~1.3–1.5. Molecular weights were higher than those achieved using SAP (25–45 kDa vs 10–20 kDa) and were reproducible. The degree of polymerization (DP) deviated, however, from that predicted from catalyst loading.

We sought to enhance the polymerization to approach a more living system by incorporating the less stable and potentially more reactive cis-olefin. The MCO, cis-Eg-(LGLM)₂, was prepared by Z-selective metathesis.⁴⁵ The enhanced selectivity of the catalyst for cis-MCO leads to more living polymerization character, as highlighted in Figure 3. Dispersities of <1.1 were maintained throughout the reaction and consistently higher molecular weights were obtained. Conversion of MCO followed linear first-order kinetics, assuming saturation conditions, 67 and >90% monomer conversion was attained in only 10 min. Over the course of the reaction, the 85-90% cis-olefin content was converted to ~85% trans in the resulting polymer. Moreover, we observed that the cis-olefin was consumed preferentially both under the polymerization conditions and in a control experiment in which equal mixtures of both isomers were exposed to catalyst

(Figures 3B and S1). Although the faster reaction of the cisisomer was not surprising based on earlier reports of *cis/trans* metathesis behavior, ⁶⁸ the true source of this preferential reactivity was not clear. To address this question, we examined the system computationally (vide infra).

Molecular Weight Control Studies. Varying catalyst (G2) loading across all monomers resulted in at least a moderate degree of molecular weight control, yet the extent varied with olefin geometry and monomer composition (Figure 4). cis-Olefin-containing MCOs displayed a near-living

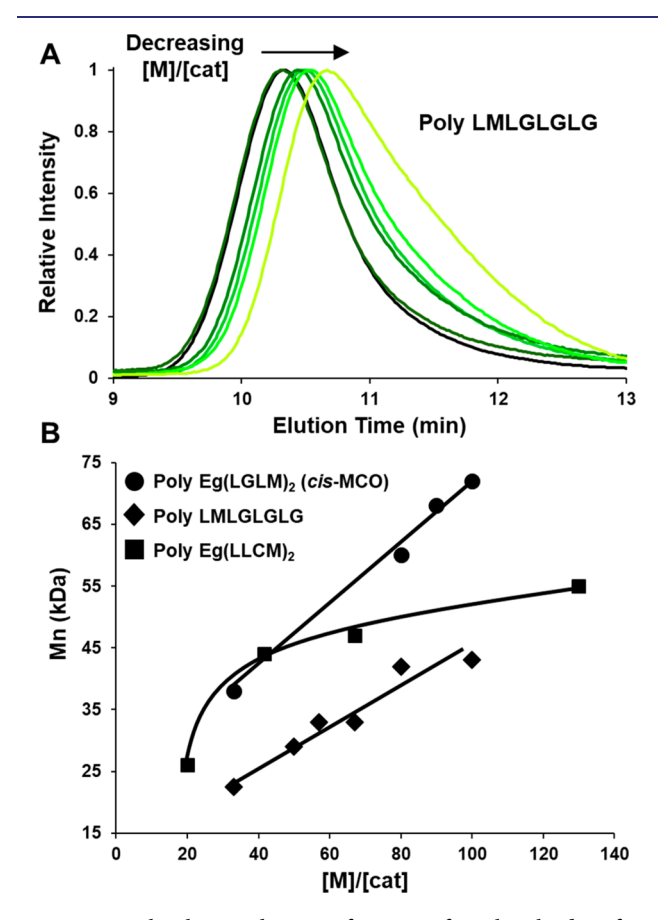


Figure 4. Molecular weights as a function of catalyst loading from palindromic monomers *trans*-Eg(LLCM)₂, *cis*-Eg(LGLM)₂, and unsymmetric *trans*-LM_{H-T}LGLGLG.

linear molecular weight control ranging from 35–70 kDa while *trans*-MCOs tracked with [M]/[cat] at high catalyst loadings but saturated with low loadings. There was also some evidence for composition dependence. *trans*-Eg(LLCM)₂ exhibited the least linear degree of control plateauing at ~55 kDa while the unsymmetric *trans*-LMLGLGLG displayed more control before saturation at 50 kDa. Although temperature would be expected to be an important factor in this entropy-controlled process, ⁶⁹ cooling the reaction (0 °C) did appear to affect molecular weight or dispersity at the relatively high concentrations being used for these experiments.

The low dispersities observed for the *cis*-MCOs suggest that we have successfully favored propagation over secondary metathesis. We believe that the slightly larger *D*'s observed at high catalyst loadings of *cis*-MCOs are due primarily to incomplete initiation in these extremely concentrated, and therefore, rapid polymerization conditions. The Interestingly, dispersities remain below the theoretically predicted 2 for

even *trans*-olefin MCOs which suggests that these systems are not achieving equilibrium before they are quenched. We are not certain why this is the case as reactions run at longer reaction times did not result in higher dispersities. Experimentally, it may be that the catalyst deteriorates before equilibrium is achieved or that the bond selectivity of the secondary metathesis reaction is not fully random. Functionally, the limit on dispersity may also be due to the relatively low DPs of these large MCOs.

Chain and Block Extensions via SEED-ROMP. As we were interested in determining the degree to which these polymerizations could be considered living, we carried out both chain extension experiments and block copolymerizations with *cis*-Eg(LGLM)₂ (Figure 5). For chain extension, an initial polymerization with a fixed amount of MCO was followed by a second addition of the same MCO. To prepare block copolymers the initial polymerization of the MCO was followed by the addition of a traditional strained ROMP monomer, norbornene (NBE), or *cis*-cyclooctene (COE).^{71–74}

The chain extension produced a polymer of higher molecular weight which maintained a D < 1.1. When the experiment was undertaken with NBE, block copolymers ranging from 60 to 90 kDa were obtained. These polymers, however, exhibited significant secondary metathesis resulting in unpredictable final molecular weights and considerable increases in dispersities (Figure 5B). Attempts to control the block formation by controlling reaction time and temperature resulted in only small improvements (Figure S3). Each time block addition was repeated, a clear increase in molecular weight with minimal increase in dispersity was observed within 1 min, but molecular weight quickly decreased and broadened in dispersity thereafter (Figure S4). However, ¹H NMR spectra remained clean in the G methylene region, indicating that the polyester block did not suffer from significant secondary metathesis and the uncontrollable molecular weights originated from the highly reactive norbornene block. It is worth mentioning that there exist many variants of functionalized norbornenes that offer more control, 75-77 but these derivatives were not investigated in this current proof of principle study. The significant increases in dispersities and small increases in molecular weights (Figures 5b and S3) could also indicate that a significant portion of chain ends were deactivated and unable to undergo block extension. To address this possibility, the experiment was repeated with COE. In this case, block addition was achieved with no increase in dispersity and molecular weights of ~70 kDa (Figure 5C). This result is consistent with the conservation of a high percentage of active chain ends. As the process would not be expected to be purely living, however, some degree of chain transfer is expected.

Although not a subject of the current work, it is worth noting that ROMP monomers such as NBE and COE may be functionalized to potentially attach deliverable payloads into biological systems for controlled release, or initiate micellar self-assembly. ^{72,78,79} SEED-ROMP is therefore an exceptionally powerful tool in engineering materials for controlled and precise function.

Catalyst Initiation Effects. Switching catalyst from the G2 catalyst to the Grubbs third generation catalyst (G3), which is known to exhibit faster initiation, 80-82 did not significantly affect the kinetics, molecular weights, or dispersities (Figure S2). Unsurprisingly, the more reactive catalyst proved less robust to contaminants.

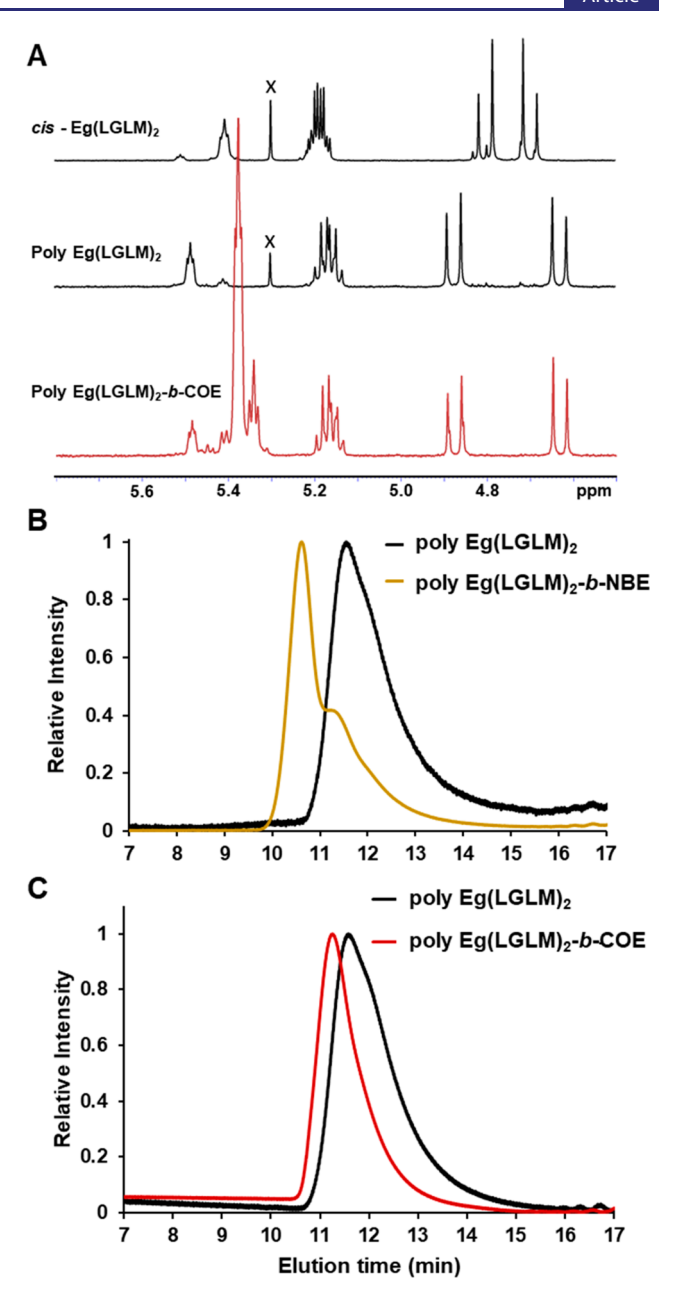


Figure 5. (A) ¹H NMR spectra for *cis*-Eg(LGLM)₂, polymerization to 50 kDa Poly Eg(LGLM)₂, and Poly Eg(LGLM)₂-*b*-COE. (× denotes CH₂Cl₂) (B) SEC traces of control and block extension using NBE (unpurified), displaying large dispersity due to secondary metathesis. (C) SEC traces of control and block extension with COE (unpurified).

Computational Studies. As the enhanced reactivity of the *cis*- relative to the *trans*-MCO is the basis for SEED-ROMP and key to the near-living nature of the polymerization, we performed computational studies to investigate the origins of the difference. A few factors are known to affect the kinetic reactivity of ROMP, including ring strain, ^{83–86} sterics, and electronic effects. However, both the *cis*- and *trans*-MCOs are expected to have very small ring strain energies, and, thus, the higher reactivity of the *cis*-isomer should not be promoted by ring-strain. In addition, the electronic and steric properties of *cis*- and *trans*-double bonds in the MCOs are similar. On the basis of the known kinetic reactivity of acyclic *cis*- and *trans*-olefins in cross-metathesis and ethenolysis, ^{68,87,88} the local

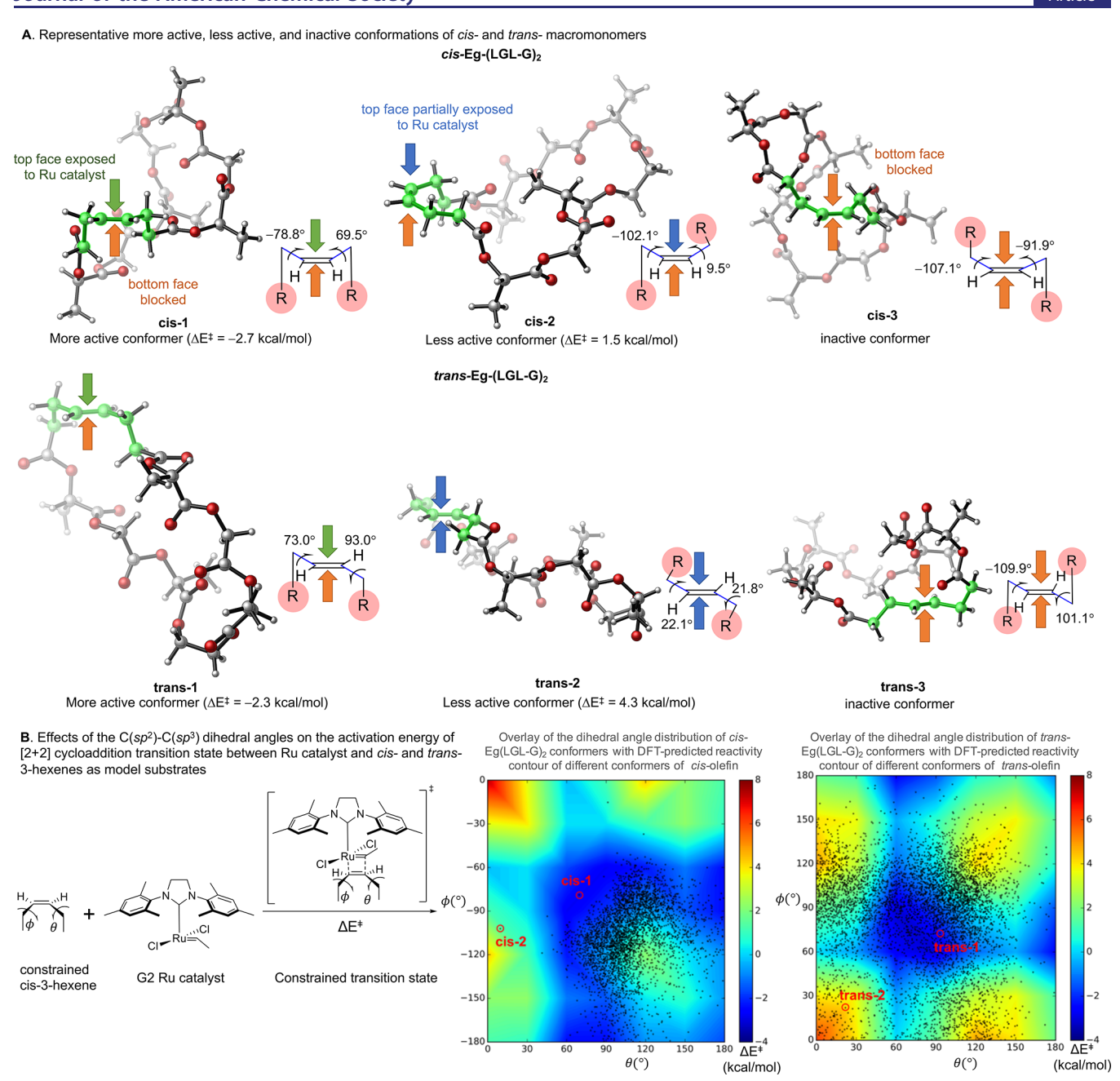


Figure 6. Molecular dynamics-density functional theory (MD-DFT) calculations. (A) Example conformations of *cis*- and *trans*-Eg(LGLM)₂. (B) Energy mapping of macrocycle conformations onto activation energy contour.

steric and electronic environments of the *cis*- and *trans*-MCOs are not expected to play a key role in differentiating their reactivities in ROMP. We surmised the conformational flexibility of the macrocyclic monomers might affect the ability of the C=C double bond to approach the Ru catalyst, which then could, in turn, affect the reactivity of *cis*- and *trans*-MCOs. Due to the flexible nature of the macrocyclic monomers, a large number of conformers exist in the resting state and many of these conformers are expected to provide access to the [2 + 2] cycloaddition transition state. Thus, a complete understanding of the relative reactivity of *cis*- versus *trans*-MCOs requires the evaluation of all ground state conformers and their relative reactivity in the [2 + 2] cycloaddition transition state.

As the large number of transition state conformers is highly challenging for conventional transition state calculations, we utilized a combined molecular dynamics/density functional theory (MD-DFT) approach to investigate the conformational flexibility of the monomers using MD trajectory simulations combined with evaluation of reactivities of each monomer conformation using DFT.

In our preliminary study, ⁴⁵ we compared the conformations of the *cis*- and *trans*-MCOs from snapshots of MD simulations with the DFT-optimized transition state geometries that used *cis*- and *trans*-3-hexene as model substrates. ⁴⁵ It was revealed that the geometries of the *cis*-MCOs have smaller deviations from the reactive olefin conformations in the metathesis transition state, indicating greater populations of metathesis-active monomers, than the *trans*-MCO. To provide a more quantitative understanding of how monomer conformation affects the metathesis reactivity, we created a model that

estimates the activation energy required for each MCO conformer to undergo [2 + 2] cycloaddition with the 14-electron Ru alkylidene complex derived from the G2 catalyst.

First, we performed 20 ns MD simulations of cis- and trans-Eg(LGLM), in a dichloroethane solvent box. Snapshots of the MD simulations revealed great levels of conformational flexibility in the two dihedral angles (θ and ϕ) for the C–C sigma bonds attached to the alkene. These conformers are expected to exhibit dramatically different reactivity in the [2 + 2] cycloaddition. Conformers with the two olefin substituents (highlighted in green in Figure 6A) placed on the same face of the double bond have exposed C=C double bonds (e.g., cis-1), which are expected to be more reactive with the catalyst. If one of the substituents is placed in the same plane of the double bond, then an increased steric repulsion with the Ru catalyst is expected, and, thus, the reactivity should be lower (e.g., cis-2). For conformers with two substituents on opposite faces, the C=C double bond is blocked for both, which translates into the lowest reactivity with G2 (e.g., cis-3). Similarly, the dihedral angles (θ and ϕ) are also expected to affect the reactivity of the conformers of the trans-MCO.

To quantify the effects of the two highlighted dihedral angles on the reactivity of the conformers, we established an activation energy contour by correlating the DFT-calculated activation energies of constrained [2+2] cycloaddition transition states (ΔE^{\ddagger}) with two varying but fixed dihedral angles $(\theta$ and ϕ) for a model system of constrained *cis*- and *trans*-alkenes. The activation energy contours were calculated using a model system of constrained *cis*- and *trans*-3-hexenes and a 14-electron Ru alkylidene complex derived from the G2 catalyst (Figure 6B). All constrained transition states were validated with the imaginary frequency vibration corresponding with the [2+2] cycloaddition process, and their activation energies were color-encoded where the blue indicated the more reactive region while the yellow to red indicated the less reactive region (Figure 6B, right).

We next mapped the *cis*- and *trans*-MCO conformers from the MD snapshots onto the generated activation energy contour. The activation energy for each conformer was thereby estimated with respect to two corresponding dihedral angles via linear interpolation from the contour. As shown in Figure 6B, the conformers of *cis*-MCO were primarily localized on the most reactive regions (blue, $\Delta E^{\ddagger} < 0$ kcal/mol) such as *cis*-1 with the estimated activation energy of -2.7 kcal/mol. Only a relatively small fraction of *cis*-conformers were in the less reactive region, colored cyan-to-yellow. For example, *cis*-2 with one dihedral angle close to 0, which makes the top face of the double bond more sterically hindered, has a higher activation energy of 1.5 kcal/mol.

In contrast, *trans*-MCOs were more flexible. The conformers are more dispersed throughout the contour map and have a greater distribution in less reactive regions than the *cis*-MCOs. For instance, *trans*-1, one of the most reactive conformers $(\Delta E^\ddagger = -2.3 \text{ kcal/mol})$, has the double bond fully exposed to Ru catalyst from the top face. *trans*-2 is less reactive $(\Delta E^\ddagger = 4.3 \text{ kcal/mol})$, however, with two olefin substitutes placed on the plane of the double bond. This arrangement increases the steric repulsion between the substitutes and the Ru catalyst in their transition state.

Our computational studies suggest that the higher reactivity of *cis*-MCOs can be attributed to their more localized conformer ensembles with the majority being reactive conformations for [2 + 2] cycloaddition in ROMP. It is

interesting to note that this finding is subtly different from the intuitive rationale that *cis*-olefins react faster because they are "more accessible" and can more easily approach the metal center. This reasoning is based on a model of the olefin in which the substituents present a singular steric profile rather than a population of profiles and does not take into account the fact that not all coordination modes lead to energetically favorable transition states.

CONCLUSIONS

We have successfully designed a general, modular, and scalable synthetic method for the preparation of copolymers in which sequence is imbedded into a large macrocycle which is then polymerized using ED-ROMP. SEED-ROMP, which exploits a more reactive *cis*-olefin metathesis handle, enhanced the living character of the polymerization, improving molecular weight control, decreasing dispersity, and facilitating the preparation of block copolymers. Computational analysis demonstrated that *cis*-olefin-containing monomers promote propagation over secondary metathesis by reacting faster than the *trans*-isomers and that the preference arises from the fact that conformationally rigid *cis*-macromonomers present a higher population of reaction-favoring binding modes.

We have also established that ring-closing via macrolactonization can be carried out at higher concentrations and less expensively than RCM-based ring-closure in the preparation of the cyclic MCOs. Moreover, the precursor oligomers required for this method do not require an additional linker group (Eg) in their construction, meaning that the final polymers more closely resemble the ideal structure for a poly(α -hydroxy acid).

The development of sequence-controlled polymer syntheses is an ongoing effort, in which homogeneity across samples in molecular weight and dispersity is critical. The current approach, which couples experimental intuition with theory, has expanded both the range of materials that can be prepared and our ability to control their characteristics. It seems likely, moreover, that this general approach will be applicable to polymers other than $poly(\alpha-hydroxy\ acid)s$; all that is required is that target sequence be incorporated into an MCO with a metathesis-active olefin. With such methods it should be possible to better target sequenced materials for future applications.

■ EXPERIMENTAL SECTION

Materials. All experiments were carried out in oven-dried glassware under an atmosphere of N_2 using standard Schlenk line techniques. N_1N' -Dicyclohexylcarbodiimide (DCC) was purchased from Oakwood Chemical and used without further purification. 1,2-dichloroethane (DCE) was purchased from Fisher and used as is. Methylene chloride (CH $_2$ Cl $_2$, Fisher), ethyl acetate (EtOAc, Sigma-Aldrich), and tetrahydrofuran (THF, Fisher) were purified by passage over neutral activated alumina. The reagents 4-(dimethylamino)-pyridinium 4-toluenesulfonate (DPTS), silyl (Si-R $_3$, tert-butyldiphenylsilyl) and benzyl (Bn) protected monomers, unprotected monomers, and polymers were prepared according to previously published protocols.

 1 H NMR Spectroscopy. 1 H (400 and 500 MHz) NMR spectra were recorded using Bruker spectrometers in CDCl₃ and calibrated to the solvent peak of δ 7.26 ppm.

Size Exclusion Chromatography. Molecular weights and dispersities were obtained on the following: (1) Waters GPC (THF) with Jordi 500, 1000, and 10000 Å divinylbenzene columns, and refractive index detector (Waters) was calibrated to polystyrene

standards; (2) TOSOH HLC-8320GPC EcoSEC equipped with two columns (TSK-3000H, TSK-4000H). A mobile phase of THF inhibited with 0.025% butylated hydroxytoluene at 40 °C was used, reported molecular weights are relative to polystyrene standards.

Differential Scanning Calorimetry. Differential scanning calorimetry was performed with TA Instruments Q200. Each run was performed at 10 $^{\circ}$ C/min heating and cooling rates. $T_{\rm g}$'s were recorded in the second heating cycle.

MALDI-oF MS. MALDI-TOF MS spectra were obtained on a Bruker ultrafleXtreme MALDI-ToF instrument. An accelerating voltage of 20 kV was applied, and spectra were obtained in reflection mode (500 shots). The polymers were dissolved in THF to yield a concentration of 1 mg/mL. Potassium trifluoroacetate (KTFA) was used as the catonization agent and was dissolved in THF to form a 1 mg/mL solution. The matrix was DCTB in THF as a 40 mg/mL solution. The three solutions were combined in a ratio of 1:1:1.5 (polymer: DCTB: KFTA) and allowed to mix for 1 h. The solution was then drop cast onto a 100-well MALDI plate and allowed to dry before analysis. Spectra were obtained using Bruker flexAnalysis software package.

trans-Selective RCM of Eg(LGLM)2-Representative Procedure. A solution of G2 (3.9 mg, 0.0046 mmol) in CH₂Cl₂ (1 mL) was added to a stirring solution of Eg(LGLM)₂ (28.0 mg, 0.044 mmol) in CH2Cl2 (42 mL) and the reaction was stirred at rt overnight. The reaction was quenched by adding ethyl vinyl ether (1 mL), and the reaction was concentrated in vacuo. The crude material was purified by flash chromatography (SiO2, 20-30% EtOAc in hexanes) to provide products as colorless liquids with E:Z ratios near 85:15 (24.1 mg, 89.9%) ¹H NMR (400 MHz, CDCl₃) δ 5.44–5.23 (trans) and 5.39-5.38 (cis) (m, 2H), 5.23 (m, 4H), 4.79 (d, J = 16.0Hz, 2H, trans), 4.77 (d, J = 16.0 Hz, 2H, cis), 4.38 (m, 4 H), 2.44 (m, 8H), 1.52 (d, J = 7.0 Hz, 6H), 1.50 (d, J = 7.0 Hz, 6H); ¹³C NMR (100 MHz, CDCl₃) δ 172.27, 172.22, 170.19, 169.76, 166.61, 129.32 (trans), 129.12 (cis), 69.35, 68.19, 62.71, 60.86, 33.62, 27.56, 27.34, 22.75, 16.85, 16.69, 16.65; HRMS (ESI) calcd. mass 603.1920, found 603,19028

cis-Selective RCM of Eg(LGLM)2. In the glovebox, a solution of GN (69 mg, 0.1094 mmol) in DCE (20 mL) was added to a stirring solution of Eg-(LGLM)₂ (690 mg, 1.094 mmol) in DCE (200 mL). The vessel was immediately removed from the glovebox and stirred at 60 °C under a constant low vacuum. After 26 h of stirring, the reaction solution was cooled to rt, ethyl vinyl ether (1 mL) was added, and the solution was concentrated. The crude product was purified by flash chromatography (SiO2, 20-30% EtOAc in hexanes) to afford cis-Eg(LGLM)₂ (0.578 g, 88% yield, 95% BRSM, 12:88 E:Z) as a colorless oil; 1 H NMR (500 MHz, CDCl₃) δ 5.51 (m, trans) and 5.43 (m, cis) (2H), 5.23 (m, 4H), 4.83 (d, J = 16.0 Hz, 2H, trans), 4.81 (d, J = 16.0 Hz, 2H, cis), 4.40 (m, 4 H), 2.48 (m, 8H), 1.55 (d, J = 7.0Hz, 6H), 1.53 (d, J = 7.0 Hz, 6H); ¹³C NMR (125 MHz, CDCl₃) δ 172.44, 170.32, 169.92, 166.77, 129.47 (trans), 129.12 (cis), 69.52, 68.34, 62.81, 60.96, 33.96, 22.91, 16.94, 16.80; HRMS (ESI) calcd. mass 603.1920, found 603.1940.

Macrolactonization-Representative Procedure. Using a syringe pump, a solution of SyLMLGLGL (1.61 g, 2.25 mmol in 25 mL DCE) was injected into a 60 °C, 225 mL solution of DCE containing DCC (0.510 g, 2.47 mmol) and DPTS (0.132 g, 0.450 mmol) over the span of 16 h. The solution was stirred for an additional 8 h before cooling to rt, filtration, and concentrating in vacuo to obtain the crude product. The crude oil was purified by flash chromatography (SiO₂, 20-30% EtOAc in hexanes) to produce the product as a white solid.; ¹H NMR (500 MHz, CDCl₃) δ 7.36 (s, 2H), 5.50 (q, J = 7.2 Hz, 1H), 5.46 (q, J = 7.2 Hz, 1H), 5.22 (q, J =7.2 Hz, 1H), 5.03 (q, J = 7.2 Hz, 1H), 4.85 (d, J = 16 Hz, 1H), 4.72 (d, J = 16 Hz, 1H), 4.68 (d, J = 16 Hz, 1H), 4.63 (d, J = 16 Hz, 1H),4.11 (t, J = 6.8 Hz, 2H), 3.85 (s, 6H), 3.16 (m, 2H), 2.35 (q, J = 6.8, 2H), 1.67 (m, 6H), 1.49 (d, J = 7.2 Hz, 3H), 1.36 (d, J = 7.2 Hz, 3H) 13 C NMR (125 MHz, CDCl₃) δ 175.65, 170.06, 169.82, 169.25, 167.90, 166.30, 166.19, 165.08, 152.09, 132.38, 129.44, 127.73, 124.51, 106.65, 69.57, 69.33, 69.07, 68.50, 64.32, 60.97, 60.42, 56.43,

37.77, 31.69, 17.02, 16.91, 16.66, 16.58; HRMS (ESI) calcd. mass 696.1880, found 696.18686.

Polymerization with G2—Representative Procedure. G2 (10.5 mg, 0.012 mmol) was dissolved in CH₂Cl₂ (0.3 mL) and added via syringe to a stirring solution of *trans*-Eg(LGLM)₂ (0.57 g, 0.94 mmol) in CH₂Cl₂ (1.0 mL). The reaction was stirred at rt for 4 h before ethyl vinyl ether was added (0.2 mL) to quench. The reaction mixture was dissolved in a minimal amount of CH₂Cl₂ and precipitated into 250 mL swirling MeOH. The off-white solid was isolated (74.8%). ¹H NMR (500 MHz, CDCl₃) δ 5.49 (m, 1.7 H; *trans*), 5.42 (m, 0.3H, *cis*), 5.20 (q, *J* = 7.5 Hz, 2H), 5.18 (q, *J* = 7.0 Hz, 2H), 4.89 (d, *J* = 16.5 Hz, 2H), 4.65 (d, *J* = 16.5 Hz, 2H), 4.41 (m, 4H), 2.50 (m, 4H), 2.35 (m, 4H), 1.56 (d, *J* = 7.0 Hz, 6H), 1.53 (d, *J* = 7.5 Hz, 6H); ¹³C NMR (125 MHz, CDCl₃) δ 172.39, 170.27, 169.75, 166.66, 129.35, 69.27, 68.17, 62.79, 60.69, 33.69, 27.58, 16.88, 16.74; DSC: T_{σ} = 18 °C.

Molecular Weight Control Studies. To investigate the degree of molecular weight control, polymers were prepared using the same conditions as described above, with varying mol % catalyst loadings to achieve the desired M/cat ratio. Solutions (1 mg/mL) of unpurified polymers were utilized for SEC analysis.

Kinetics Study. To a stirring solution of *cis*-Eg-(LGLM)₂ (72 mg, 120 μ mol) and CH₂Cl₂ (121 μ L) was added a solution of catalyst G2 (1.3 mg, 1.5 μ mol) in CH₂Cl₂ (50 μ L). Aliquots were removed via pipet at the specified time points and added to a vial containing a solution of ethyl vinyl ether to quench the catalyst. The *cis*-to-*trans* ratio of monomer was approximated by comparing peak integrations at 4.85–4.75 ppm. Total conversion was approximated by comparing peak integrations at 4.9–4.75 ppm.

SEED-ROMP Block Extensions—Representative Procedure. A solution of G2 (0.18 mg, 0.218 μ mol) in CH₂Cl₂ (10 μ L) was added to a premixed solution of cis-Eg(LGLM)₂ (10.5 mg, 17.4 μ mol) in CH₂Cl₂ (15 μ L) and allowed to shake for 10 min before a premixed solution of NBE (41 mg, 435 μ mol) in CH₂Cl₂ (25 μ L) was added at room temperature. The vial was shaken for 1 min, and EVE was added and was shaken for an additional 10 min. The mixture was diluted to a preweighed vial after diluting with CH2Cl2 (0.3 mL) and concentrated in vacuo to provide crude poly Eg(LGLM)₂-b-NBE as a solid (18.5 mg, 93% SEED-ROMP monomer conversion, 64% cisolefin incorporation in poly(NBE); based on DP, composition is 46 mol % block A (poly Eg(LGLM)₂, DP 100) and 54 mol % block B (polyNBE, DP 117). To add clarity to integration numbers presented herein, a 50:50 ratio of A:B has been assigned, and a 50:50 cis:trans ratio has been assigned for the NBE block. ¹H NMR (500 MHz, CDCl₃) δ 5.51 (m) and 1.42 (m) (2H), 5.35 (br s, 1H) and 5.21 (m, 5H), 4.89 (d, J = 16.0 Hz, 2H), 4.65 (d, J = 16.5 Hz, 2H), 4.41 (m, 4H), 2.85 (br s, 2H), 2.50 (m, 5H), 2.33 (m, 4H), 1.87 (m, 1H), 1.80 (m, 2H) 1.55 (d, J = 6.0 Hz, 6H), 1.53 (d, J = 7.0 Hz, 6H) 1.35 (m, 2H)2H), 1.09 (m, 1H); 13 C NMR (125 MHz, CDCl₃) δ 172.49, 170.38, 169.86, 166.78, 134.14, 134.07, 134.03, 133.99, 133.90, 133.28, 133.15, 1300, 129.49, 129.154, 129.04, 69.41, 68.36, 68.30, 62.92, 60.83, 43.56, 43.27, 42.90, 42.24, 38.81, 38.56, 33.84, 33.25, 33.07, 32.52, 32.36, 27.72, 17.02, 16.88; SEC (THF): $M_p = 71.4 \text{ kDa}$, $M_w = 71.4 \text{ kDa}$ 78.8 kDa, D = 1.10.

ASSOCIATED CONTENT

S Supporting Information

The Supporting Information is available free of charge on the ACS Publications website at DOI: 10.1021/jacs.8b13120.

Complete experimental details, spectral data, and supplementary figures (PDF)

AUTHOR INFORMATION

Corresponding Author

*tmeyer@pitt.edu

ORCID

Cheng Fang: 0000-0002-9767-2043

Peng Liu: 0000-0002-8188-632X Tara Y. Meyer: 0000-0002-9810-454X

Funding

NSF CHE-1410119, NSF CHE-1709144, NIH GM128779, and CHE-1625002 for MALDI-ToF instrumentation.

Notes

The authors declare no competing financial interest.

ACKNOWLEDGMENTS

T.Y.M. acknowledges NSF CHE-1410119, NSF CHE-1709144, NSF CHE-1625002, and the University of Pittsburgh for financial support. P.L. thanks the NIH (GM128779) for financial support for this work. P.L. acknowledges supercomputer resources provided by the Center for Research Computing at the University of Pittsburgh and the Extreme Science and Engineering Discovery Environment (XSEDE) supported by the NSF.

REFERENCES

- (1) Swisher, J. H.; Nowalk, J. A.; Washington, M. A.; Meyer, T. Y. Properties and Applications of Sequence-Controlled Polymers. In Sequence-Controlled Polymers; Wiley-VCH Verlag GmbH & Co. KGaA: 2018; pp 435–478.
- (2) Amonoo, J. A.; Li, A.; Purdum, G. E.; Sykes, M. E.; Huang, B.; Palermo, E. F.; McNeil, A. J.; Shtein, M.; Loo, Y.-L.; Green, P. F. An all-conjugated gradient copolymer approach for morphological control of polymer solar cells. *J. Mater. Chem. A* **2015**, 3 (40), 20174–20184.
- (3) Klumperman, B. Statistical, Alternating and Gradient Copolymers. In *Macromolecular Engineering*; Wiley-VCH Verlag GmbH & Co. KGaA: 2007; pp 813–838.
- (4) van Zoelen, W.; Zuckermann, R. N.; Segalman, R. A. Tunable Surface Properties from Sequence-Specific Polypeptoid—Polystyrene Block Copolymer Thin Films. *Macromolecules* **2012**, *45* (17), 7072—7082
- (5) Hosono, N.; Gillissen, M. A. J.; Li, Y.; Sheiko, S. S.; Palmans, A. R. A.; Meijer, E. W. Orthogonal Self-Assembly in Folding Block Copolymers. J. Am. Chem. Soc. 2013, 135 (1), 501–510.
- (6) Schmidt, B. V. K. J.; Fechler, N.; Falkenhagen, J.; Lutz, J.-F. Controlled folding of synthetic polymer chains through the formation of positionable covalent bridges. *Nat. Chem.* **2011**, 3 (3), 234–238.
- (7) Murnen, H. K.; Khokhlov, A. R.; Khalatur, P. G.; Segalman, R. A.; Zuckermann, R. N. Impact of Hydrophobic Sequence Patterning on the Coil-to-Globule Transition of Protein-like Polymers. *Macromolecules* **2012**, *45* (12), 5229–5236.
- (8) Cole, J. P.; Hanlon, A. M.; Rodriguez, K. J.; Berda, E. B. Proteinlike structure and activity in synthetic polymers. *J. Polym. Sci., Part A: Polym. Chem.* **2017**, 55 (2), 191–206.
- (9) Grate, J. W.; Mo, K.-F.; Daily, M. D. Triazine-Based Sequence-Defined Polymers with Side-Chain Diversity and Backbone-Backbone Interaction Motifs. *Angew. Chem., Int. Ed.* **2016**, *55* (12), 3925–3930.
- (10) Lee, H.; Hoshino, Y.; Wada, Y.; Arata, Y.; Maruyama, A.; Miura, Y. Minimization of Synthetic Polymer Ligands for Specific Recognition and Neutralization of a Toxic Peptide. *J. Am. Chem. Soc.* **2015**, *137* (34), 10878–10881.
- (11) Mahon, C. S.; Fulton, D. A. Mimicking nature with synthetic macromolecules capable of recognition. *Nat. Chem.* **2014**, *6* (8), 665–672.
- (12) Lutz, J.-F.; Ouchi, M.; Liu, D. R.; Sawamoto, M. Sequence-Controlled Polymers. *Science* **2013**, 341 (6146), 1238149.
- (13) Chile, L.-E.; Mehrkhodavandi, P.; Hatzikiriakos, S. G. A Comparison of the Rheological and Mechanical Properties of Isotactic, Syndiotactic, and Heterotactic Poly(lactide). *Macromolecules* **2016**, 49 (3), 909–919.

- (14) Södergård, A.; Stolt, M. Properties of lactic acid based polymers and their correlation with composition. *Prog. Polym. Sci.* **2002**, *27* (6), 1123–1163.
- (15) van Zoelen, W.; Buss, H. G.; Ellebracht, N. C.; Lynd, N. A.; Fischer, D. A.; Finlay, J.; Hill, S.; Callow, M. E.; Callow, J. A.; Kramer, E. J.; Zuckermann, R. N.; Segalman, R. A. Sequence of Hydrophobic and Hydrophilic Residues in Amphiphilic Polymer Coatings Affects Surface Structure and Marine Antifouling/Fouling Release Properties. ACS Macro Lett. 2014, 3 (4), 364–368.
- (16) Heo, H.; Kim, H.; Lee, D.; Jang, S.; Ban, L.; Lim, B.; Lee, J.; Lee, Y. Regioregular D1-A-D2-A Terpolymer with Controlled Thieno[3,4-b]thiophene Orientation for High-Efficiency Polymer Solar Cells Processed with Nonhalogenated Solvents. *Macromolecules* **2016**, 49 (9), 3328–3335.
- (17) Tsai, C.-H.; Fortney, A.; Qiu, Y.; Gil, R. R.; Yaron, D.; Kowalewski, T.; Noonan, K. J. T. Conjugated Polymers with Repeated Sequences of Group 16 Heterocycles Synthesized through Catalyst-Transfer Polycondensation. *J. Am. Chem. Soc.* **2016**, *138* (21), 6798–6804.
- (18) Middleton, L. R.; Trigg, E. B.; Schwartz, E.; Opper, K. L.; Baughman, T. W.; Wagener, K. B.; Winey, K. I. Role of Periodicity and Acid Chemistry on the Morphological Evolution and Strength in Precise Polyethylenes. *Macromolecules* **2016**, 49 (21), 8209–8218.
- (19) Zhang, S.; Bauer, N. E.; Kanal, I. Y.; You, W.; Hutchison, G. R.; Meyer, T. Y. Sequence Effects in Donor–Acceptor Oligomeric Semiconductors Comprising Benzothiadiazole and Phenylenevinylene Monomers. *Macromolecules* **2017**, *50* (1), 151–161.
- (20) Bischof, A. M.; Zhang, S.; Meyer, T. Y.; Lear, B. J. Quantitative Assessment of the Connection between Steric Hindrance and Electronic Coupling in 2,5-Bis(alkoxy)benzene-Based Mixed-Valence Dimers. *J. Phys. Chem. C* **2014**, *118* (24), 12693–12699.
- (21) Sun, J.; Teran, A. A.; Liao, X.; Balsara, N. P.; Zuckermann, R. N. Crystallization in Sequence-Defined Peptoid Diblock Copolymers Induced by Microphase Separation. *J. Am. Chem. Soc.* **2014**, *136* (5), 2070–2077.
- (22) Sun, J.; Stone, G. M.; Balsara, N. P.; Zuckermann, R. N. Structure-Conductivity Relationship for Peptoid-Based PEO-Mimetic Polymer Electrolytes. *Macromolecules* **2012**, *45* (12), 5151–5156.
- (23) Aitken, B. S.; Wieruszewski, P. M.; Graham, K. R.; Reynolds, J. R.; Wagener, K. B. Control of Charge-Carrier Mobility via In-Chain Spacer Length Variation in Sequenced Triarylamine Functionalized Polyolefins. ACS Macro Lett. 2012, 1 (2), 324–327.
- (24) Li, J.; Rothstein, S. N.; Little, S. R.; Edenborn, H. M.; Meyer, T. Y. The Effect of Monomer Order on the Hydrolysis of Biodegradable Poly(lactic-co-glycolic acid) Repeating Sequence Copolymers. *J. Am. Chem. Soc.* **2012**, *134* (39), 16352–16359.
- (25) Washington, M. A.; Swiner, D. J.; Bell, K. R.; Fedorchak, M. V.; Little, S. R.; Meyer, T. Y. The impact of monomer sequence and stereochemistry on the swelling and erosion of biodegradable poly(lactic-co-glycolic acid) matrices. *Biomaterials* **2017**, *117*, 66–76.
- (26) Washington, M. A.; Balmert, S. C.; Fedorchak, M. V.; Little, S. R.; Watkins, S. C.; Meyer, T. Y. Monomer sequence in PLGA microparticles: Effects on acidic microclimates and in vivo inflammatory response. *Acta Biomater.* **2018**, *65*, 259–271.
- (27) Kapoor, D. N.; Bhatia, A.; Kaur, R.; Sharma, R.; Kaur, G.; Dhawan, S. PLGA: a unique polymer for drug delivery. *Ther. Delivery* **2015**, 6 (1), 41-58.
- (28) Gentile, P.; Chiono, V.; Carmagnola, I.; Hatton, V. P. An Overview of Poly(lactic-co-glycolic) Acid (PLGA)-Based Biomaterials for Bone Tissue Engineering. *Int. J. Mol. Sci.* **2014**, *15* (3), 3640.
- (29) Makadia, H. K.; Siegel, S. J. Poly Lactic-co-Glycolic Acid (PLGA) as Biodegradable Controlled Drug Delivery Carrier. *Polymers* **2011**, 3 (3), 1377–1397.
- (30) Shi, X.; Wang, Y.; Ren, L.; Gong, Y.; Wang, D.-A. Enhancing Alendronate Release from a Novel PLGA/Hydroxyapatite Microspheric System for Bone Repairing Applications. *Pharm. Res.* **2009**, *26* (2), 422–430.

- (31) Jain, R. A. The manufacturing techniques of various drug loaded biodegradable poly(lactide-co-glycolide) (PLGA) devices. *Biomaterials* **2000**, *21* (23), 2475–2490.
- (32) Anderson, J. M.; Shive, M. S. Biodegradation and biocompatibility of PLA and PLGA microspheres. *Adv. Drug Delivery Rev.* 1997, 28 (1), 5–24.
- (33) Xue, Z.; Mayer, M. F. Entropy-driven ring-opening olefin metathesis polymerizations of macrocycles. *Soft Matter* **2009**, *5* (23), 4600–4611.
- (34) Gautrot, J. E.; Zhu, X. X. High molecular weight bile acid and ricinoleic acid-based copolyesters via entropy-driven ring-opening metathesis polymerisation. *Chem. Commun.* **2008**, *14*, 1674–1676.
- (35) Peng, Y.; Decatur, J.; Meier, M. A. R.; Gross, R. A. Ring-Opening Metathesis Polymerization of a Naturally Derived Macrocyclic Glycolipid. *Macromolecules* **2013**, *46* (9), 3293–3300.
- (36) Strandman, S.; Gautrot, J. E.; Zhu, X. X. Recent advances in entropy-driven ring-opening polymerizations. *Polym. Chem.* **2011**, *2*, 791–799.
- (37) Martinez, H.; Ren, N.; Matta, M. E.; Hillmyer, M. A. Ring-opening metathesis polymerization of 8-membered cyclic olefins. *Polym. Chem.* **2014**, *5* (11), 3507–3532.
- (38) Zhang, J.; Matta, M. E.; Hillmyer, M. A. Synthesis of Sequence-Specific Vinyl Copolymers by Regioselective ROMP of Multiply Substituted Cyclooctenes. *ACS Macro Lett.* **2012**, *1* (12), 1383–1387.
- (39) Martinez, H.; Miró, P.; Charbonneau, P.; Hillmyer, M. A.; Cramer, C. J. Selectivity in Ring-Opening Metathesis Polymerization of Z-Cyclooctenes Catalyzed by a Second-generation Grubbs Catalyst. *ACS Catal.* **2012**, 2 (12), 2547–2556.
- (40) Kobayashi, S.; Pitet, L. M.; Hillmyer, M. A. Regio- and Stereoselective Ring-Opening Metathesis Polymerization of 3-Substituted Cyclooctenes. *J. Am. Chem. Soc.* **2011**, *133* (15), 5794–5797.
- (41) Gautrot, J. E.; Zhu, X. X. Main-Chain Bile Acid Based Degradable Elastomers Synthesized by Entropy-Driven Ring-Opening Metathesis Polymerization. *Angew. Chem.* **2006**, *118* (41), 7026–7028.
- (42) Zhang, J.; Li, G.; Sampson, N. S. Incorporation of Large Cycloalkene Rings into Alternating Copolymers Allows Control of Glass Transition and Hydrophobicity. *ACS Macro Lett.* **2018**, *7* (9), 1068–1072.
- (43) Swisher, J. H.; Nowalk, J. A.; Meyer, T. Y. Property impact of common linker segments in sequence-controlled polyesters. *Polym. Chem.* **2019**, *10*, 244.
- (44) Weiss, R. M.; Short, A. L.; Meyer, T. Y. Sequence-Controlled Copolymers Prepared via Entropy-Driven Ring-Opening Metathesis Polymerization. *ACS Macro Lett.* **2015**, *4* (9), 1039–1043.
- (45) Short, A. L.; Fang, C.; Nowalk, J. A.; Weiss, R. M.; Liu, P.; Meyer, T. Y. Cis-Selective Metathesis to Enhance the Living Character of Ring-Opening Polymerization: An Approach to Sequenced Copolymers. ACS Macro Lett. 2018, 7, 858–862.
- (46) Hodge, P. Entropically Driven Ring-Opening Polymerization of Strainless Organic Macrocycles. *Chem. Rev.* **2014**, *114* (4), 2278–2312
- (47) Hodge, P.; Kamau, S. D. Entropically Driven Ring-Opening-Metathesis Polymerization of Macrocyclic Olefins with 21–84 Ring Atoms. *Angew. Chem., Int. Ed.* **2003**, 42 (21), 2412–2414.
- (48) Tastard, C. Y.; Hodge, P.; Ben-Haida, A.; Dobinson, M. Entropically driven ring-opening metathesis polymerization (ED-ROMP) of macrocyclic olefin-containing oligoamides. *React. Funct. Polym.* **2006**, *66* (1), 93–107.
- (49) Deng, L.-L.; Guo, L.-X.; Lin, B.-P.; Zhang, X.-Q.; Sun, Y.; Yang, H. An entropy-driven ring-opening metathesis polymerization approach towards main-chain liquid crystalline polymers. *Polym. Chem.* **2016**, *7* (33), 5265–5272.
- (50) Chatterjee, A. K.; Choi, T.-L.; Sanders, D. P.; Grubbs, R. H. A General Model for Selectivity in Olefin Cross Metathesis. *J. Am. Chem. Soc.* **2003**, *125* (37), 11360–11370.
- (51) Weiss, R. M.; Jones, E. M.; Shafer, D. E.; Stayshich, R. M.; Meyer, T. Y. Synthesis of repeating sequence copolymers of lactic,

- glycolic, and caprolactic acids. J. Polym. Sci., Part A: Polym. Chem. 2011, 49 (8), 1847–1855.
- (52) Keitz, B. K.; Endo, K.; Patel, P. R.; Herbert, M. B.; Grubbs, R. H. Improved Ruthenium Catalysts for Z-Selective Olefin Metathesis. *J. Am. Chem. Soc.* **2012**, *134* (1), 693–699.
- (53) Fandrick, K. R.; Savoie, J.; Yee, N.; Song, J. J.; Senanayake, C. H. Challenges and Opportunities for Scaling the Ring-Closing Metathesis Reaction in the Pharmaceutical Industry. In *Olefin Metathesis*; John Wiley & Sons, Inc.: 2014; pp 349–365.
- (54) Boden, E. P.; Keck, G. E. Proton-transfer steps in Steglich esterification: a very practical new method for macrolactonization. *J. Org. Chem.* **1985**, *50* (13), 2394–2395.
- (55) Levengood, M. R.; Zhang, X.; Hunter, J. H.; Emmerton, K. K.; Miyamoto, J. B.; Lewis, T. S.; Senter, P. D. Orthogonal Cysteine Protection Enables Homogeneous Multi-Drug Antibody—Drug Conjugates. *Angew. Chem.***2017**, *129* (3), 751–755.
- (56) Phillips, S.; Holdsworth, D.; Kauppinen, P.; Mac Namara, C. Palladium Impurity Removal from Active Pharmaceutical Ingredient Process Streams. *Johnson Matthey Technol. Rev.* **2016**, 60 (4), 277–286
- (57) Lambeth, R. H.; Pederson, S. J.; Baranoski, M.; Rawlett, A. M. Methods for removal of residual catalyst from polymers prepared by ring opening metathesis polymerization. *J. Polym. Sci., Part A: Polym. Chem.* **2010**, 48 (24), 5752–5757.
- (58) Wheeler, P.; Phillips, J. H.; Pederson, R. L. Scalable Methods for the Removal of Ruthenium Impurities from Metathesis Reaction Mixtures. *Org. Process Res. Dev.* **2016**, *20* (7), 1182–1190.
- (59) Nguyen, H. T. H.; Short, G. N.; Qi, P.; Miller, S. A. Copolymerization of lactones and bioaromatics via concurrent ring-opening polymerization/polycondensation. *Green Chem.* **2017**, *19*, 1877
- (60) Stayshich, R. M.; Meyer, T. Y. New Insights into Poly(lactic-coglycolic acid) Microstructure: Using Repeating Sequence Copolymers To Decipher Complex NMR and Thermal Behavior. *J. Am. Chem. Soc.* **2010**, *1*32 (31), 10920–10934.
- (61) Zhang, J.; Matta, M. E.; Martinez, H.; Hillmyer, M. A. Precision Vinyl Acetate/Ethylene (VAE) Copolymers by ROMP of Acetoxy-Substituted Cyclic Alkenes. *Macromolecules* **2013**, *46* (7), 2535–2543.
- (62) Gutekunst, W. R.; Hawker, C. J. A General Approach to Sequence-Controlled Polymers Using Macrocyclic Ring Opening Metathesis Polymerization. *J. Am. Chem. Soc.* **2015**, *137* (25), 8038–8041.
- (63) Chang, A. B.; Miyake, G. M.; Grubbs, R. H. Sequence-Controlled Polymers by Ruthenium-Mediated Ring-Opening Metathesis Polymerization. In *Sequence-Controlled Polymers: Synthesis, Self-Assembly, and Properties*; American Chemical Society: 2014; Vol. 1170, pp 161–188.
- (64) Farrell, W. S.; Beers, K. L. Ring-Opening Metathesis Polymerization of Butyl-Substituted trans-Cyclooctenes. *ACS Macro Lett.* **2017**, *6* (8), 791–795.
- (65) Parker, K. A.; Sampson, N. S. Precision Synthesis of Alternating Copolymers via Ring-Opening Polymerization of 1-Substituted Cyclobutenes. *Acc. Chem. Res.* **2016**, *49* (3), 408–417.
- (66) Weiss, R. M.; Li, J.; Liu, H. H.; Washington, M. A.; Giesen, J. A.; Grayson, S. M.; Meyer, T. Y. Determining Sequence Fidelity in Repeating Sequence Poly(lactic-co-glycolic acid)s. *Macromolecules* **2017**, *50* (2), 550–560.
- (67) Sanford, M. S.; Love, J. A.; Grubbs, R. H. Mechanism and Activity of Ruthenium Olefin Metathesis Catalysts. *J. Am. Chem. Soc.* **2001**, *123* (27), 6543–6554.
- (68) Anderson, D. R.; Ung, T.; Mkrtumyan, G.; Bertrand, G.; Grubbs, R. H.; Schrodi, Y. Kinetic Selectivity of Olefin Metathesis Catalysts Bearing Cyclic (Alkyl)(Amino)Carbenes. *Organometallics* **2008**, 27 (4), 563–566.
- (69) Neary, W. J.; Kennemur, J. G. Variable Temperature ROMP: Leveraging Low Ring Strain Thermodynamics To Achieve Well-Defined Polypentenamers. *Macromolecules* **2017**, *50* (13), 4935–4941.

- (70) Dias, E. L.; Nguyen, S. T.; Grubbs, R. H. Well-Defined Ruthenium Olefin Metathesis Catalysts: Mechanism and Activity. *J. Am. Chem. Soc.* **1997**, *119* (17), 3887–3897.
- (71) Maynard, H. D.; Okada, S. Y.; Grubbs, R. H. Synthesis of Norbornenyl Polymers with Bioactive Oligopeptides by Ring-Opening Metathesis Polymerization. *Macromolecules* **2000**, 33 (17), 6239–6248.
- (72) Sutthasupa, S.; Shiotsuki, M.; Matsuoka, H.; Masuda, T.; Sanda, F. Ring-Opening Metathesis Block Copolymerization of Amino Acid Functionalized Norbornene Monomers. Effects of Solvent and pH on Micelle Formation. *Macromolecules* **2010**, 43 (4), 1815–1822.
- (73) Floros, G.; Saragas, N.; Paraskevopoulou, P.; Psaroudakis, N.; Koinis, S.; Pitsikalis, M.; Hadjichristidis, N.; Mertis, K. Ring Opening Metathesis Polymerization of Norbornene and Derivatives by the Triply Bonded Ditungsten Complex Na[W2(μ -Cl)3Cl4(THF)2]·(THF)3. *Polymers* **2012**, *4* (4), 1657–1673.
- (74) Gringolts, M. L.; Denisova, Y. I.; Shandryuk, G. A.; Krentsel, L. B.; Litmanovich, A. D.; Finkelshtein, E. S.; Kudryavtsev, Y. V. Synthesis of norbornene-cyclooctene copolymers by the crossmetathesis of polynorbornene with polyoctenamer. *RSC Adv.* **2015**, 5 (1), 316–319.
- (75) Ahmed, S. R.; Bullock, S. E.; Cresce, A. V.; Kofinas, P. Polydispersity control in ring opening metathesis polymerization of amphiphilic norbornene diblock copolymers. *Polymer* **2003**, *44* (17), 4943–4948.
- (76) Liu, Z.; Rainier, J. D. Regioselective Ring-Opening/Cross-Metathesis Reactions of Norbornene Derivatives with Electron-Rich Olefins. *Org. Lett.* **2005**, *7* (1), 131–133.
- (77) Schwab, P.; Grubbs, R. H.; Ziller, J. W. Synthesis and Applications of RuCl2(CHR')(PR3)2: The Influence of the Alkylidene Moiety on Metathesis Activity. *J. Am. Chem. Soc.* **1996**, 118 (1), 100–110.
- (78) Patel, P. R.; Kiser, R. C.; Lu, Y. Y.; Fong, E.; Ho, W. C.; Tirrell, D. A.; Grubbs, R. H. Synthesis and Cell Adhesive Properties of Linear and Cyclic RGD Functionalized Polynorbornene Thin Films. *Biomacromolecules* **2012**, *13* (8), 2546–2553.
- (79) Maynard, H. D.; Okada, S. Y.; Grubbs, R. H. Inhibition of Cell Adhesion to Fibronectin by Oligopeptide-Substituted Polynorbornenes. *J. Am. Chem. Soc.* **2001**, *123* (7), 1275–1279.
- (80) Choi, T.-L.; Grubbs, R. H. Controlled Living Ring-Opening-Metathesis Polymerization by a Fast-Initiating Ruthenium Catalyst. *Angew. Chem., Int. Ed.***2003**, 42 (15), 1743–1746.
- (81) Polymeropoulos, G.; Zapsas, G.; Ntetsikas, K.; Bilalis, P.; Gnanou, Y.; Hadjichristidis, N. 50th Anniversary Perspective: Polymers with Complex Architectures. *Macromolecules* **2017**, *50* (4), 1253–1290.
- (82) Walsh, D. J.; Lau, S. H.; Hyatt, M. G.; Guironnet, D. Kinetic Study of Living Ring-Opening Metathesis Polymerization with Third-Generation Grubbs Catalysts. *J. Am. Chem. Soc.* **2017**, *139* (39), 13644–13647.
- (83) Song, A.; Lee, J. C.; Parker, K. A.; Sampson, N. S. Scope of the Ring-Opening Metathesis Polymerization (ROMP) Reaction of 1-Substituted Cyclobutenes. *J. Am. Chem. Soc.* **2010**, *132* (30), 10513–10520.
- (84) Rowley, C. N.; van der Eide, E. F.; Piers, W. E.; Woo, T. K. DFT Study of the Isomerization and Spectroscopic/Structural Properties of Ruthenacyclobutane Intermediates Relevant to Olefin Metathesis. *Organometallics* **2008**, *27* (23), 6043–6045.
- (85) Lopez, S. A.; Houk, K. N. Alkene Distortion Energies and Torsional Effects Control Reactivities, and Stereoselectivities of Azide Cycloadditions to Norbornene and Substituted Norbornenes. *J. Org. Chem.* **2013**, 78 (5), 1778–1783.
- (86) Adlhart, C.; Chen, P. Mechanism and Activity of Ruthenium Olefin Metathesis Catalysts: The Role of Ligands and Substrates from a Theoretical Perspective. *J. Am. Chem. Soc.* **2004**, *126* (11), 3496–3510.
- (87) Benitez, D.; Tkatchouk, E.; Goddard, W. A., Iii Relevance of cis- and trans-dichloride Ru intermediates in Grubbs-II olefin

- metathesis catalysis (H2IMesCl2Ru—CHR). Chem. Commun. 2008, No. 46, 6194-6196.
- (88) Bahri-Laleh, N.; Credendino, R.; Cavallo, L. The intriguing modeling of cis-trans selectivity in ruthenium-catalyzed olefin metathesis. *Beilstein J. Org. Chem.* **2011**, *7*, 40–45.